COMPOSITIONAL VARIATION OF A VERMICULITE AS RELATED TO PARTICLE SIZE

by

RAYMOND L. KERNS, Jr. and CHARLES J. MANKIN

Oklahoma Geological Survey, University of Oklahoma, Norman, Oklahoma
and
Director, School of Geology, University of Oklahoma, Norman, Oklahoma

ABSTRACT

A VERMICULITE regolith sample from Llano, County, Texas, was divided into 16–32, 8–16, 4–8, 2–4, 1–2, $\frac{1}{2}$–1, $\frac{1}{4}$–$\frac{1}{2}$, $\frac{1}{10}$–$\frac{1}{4}$, and $\frac{5}{100}$–$\frac{1}{10}$ micron equivalent spherical diameter size-classes. A well-crystallized vermiculite found in association with the regolith was ground to −400 mesh.

The samples were analyzed by X-ray diffractometry and differential thermal analysis, and cation exchange capacity measurements were made for selected size fractions. Chemical analyses by X-ray fluorescence revealed a systematic increase in silicon with decreasing particle size. An increase in the iron content and a decrease in magnesium were also directly correlated to a decrease in the crystallite size. Aluminum content was constant throughout the range of particle sizes.

X-ray analyses showed that the coarser particles were trioctahedral, whereas the smaller crystallites were dioctahedral. These data were supported by recast formulae based on the chemical analyses. The recast formulae were substantiated by DTA and cation exchange capacity data as being reasonable approximations of actual formulae.

These observations are interpreted as an expression of chemical alteration that clay minerals may undergo in an aqueous environment. The crystallographic, cation exchange capacity, DTA, and swelling properties are a function of the chemical composition of the crystallites. Chemical composition of the crystallites is shown to be directly correlated to particle size.

INTRODUCTION

THE vermiculite samples selected for this study were collected at stop number twelve (Carl Moss Ranch) near Llano, Texas, on the field trip led by Folk as a part of the Tenth National Clay Conference.

One sample consisted of large books of yellowish-brown crystals that were found concentrated in veinlets. The average crystal sizes are about 1–2 in. in diameter. The other sample existed as loose regolith in which the individual crystal sizes range from about 3 mm to clay-sized particles. The vermiculite occurs associated with soapstone and talc, and has formed under hydrothermal conditions. Persons interested in the geology of the area are referred to the study by Clabaugh and Barnes (1959), which provides a

detailed discussion of the geology, petrology, and occurrence of vermiculites in Llano, Texas.

The sample of coarse crystals of vermiculite were prepared for study by grinding to −400 mesh size in a uniform particle size grinder. The vermiculite regolith sample was size-fractioned by Stokes' settling and continuous-flow super centrifugation into 16–32, 8–16, 4–8, 2–4, 1–2, $\frac{1}{2}$–1, $\frac{1}{4}$–$\frac{1}{2}$, $\frac{1}{10}$–$\frac{1}{4}$, and $\frac{5}{100}$–$\frac{1}{10}$ microns equivalent spherical diameters (ESD) size-classes. Distilled water was used as a dispersant and the collected materials were oven dried at 60°C, ground to −100 mesh powders, and stored in glass vials until analyzed.

Chemical analyses by X-ray fluorescence, X-ray diffractometry, cation exchange capacity determination, and differential thermal analysis data were utilized to characterize each sample.

X-RAY DIFFRACTION DATA

X-ray diffraction data for a randomly oriented powder of the large yellowish-brown crystals (ground to −400 mesh) are listed in Table 1 and are compared with the X-ray data reported by Walker (1961) for batavite and a vermiculite from West Chester, Pennsylvania. The chemical compositions of these three vermiculites are quite different, but are not indicated by differences in the X-ray diffraction powder data. Only a few of the weaker lines observed in the two samples reported by Walker were not observed in the Llano vermiculite. In particular, attention is called to the d-values of the 060 lines from which the b-axis parameter may be calculated. This is 9.22 Å for batavite and the West Chester vermiculite and 9.24 Å for the sample from the Carl Moss Ranch.

Powder data were also obtained for samples of the size-fractioned sample of vermiculite regolith. The powder data for the 16–32 microns fraction agree well with the data listed in Table 1. The differences are mainly the absence of some of the weaker diffraction lines. This loss of lines continues progressively through to the smallest size fraction. A significant change of d–values is not observed, however, until the particle size becomes less than 1 micron. This effect may be observed in the diffractometer traces of the 1–2 and $\frac{5}{100}$–$\frac{1}{10}$ micron fractions and in the data listed in Table 2. In the less than 1 micron fractions the 060 diffraction peak is not observed. A shift of the (02l), (11l) edge from 19.3° to 19.7° 2θ suggests a dioctahedral structure for the less than one micron samples.

All size-fractions of the vermiculite were prepared as sedimented slides. An equal amount of each particle size was accurately weighed, dispersed in a few drops of distilled water, and all the dispersed material placed on glass slides. All the sedimented materials were humidified at 50% relative humidity for 8 hr and scanned on a diffractometer from 2° to 90° 2θ. A total of eleven orders of the 002 reflection were observed on the 16–32 microns X-ray diffraction pattern. Finer fractions down to the less than 1 micron material have seven observable orders. For the finest fractions only five orders are

TABLE 1.—X-RAY DATA FOR SELECTED WELL-CRYSTALLIZED VERMICULITE

Indices	Batavite*		West Chester* vermiculite		Llano vermiculite large crystals	
	d(Å)	I est.	d(Å)	I est.	d(Å)	$I/I_0 \times 100$
002	14.4	vvs	14.4	vvs	14.39	100
004	7.18	vvw	7.20	vw	7.19	3
006	4.79	vw	4.79	vw	4.80	5
02l; 11l	4.60	s	4.60	s	4.61	1
008	3.602	m	3.587	m	3.59	10
0, 0, 10	2.873	m	2.869	m	2.87	13
130; 200; 20$\bar{2}$	2.657	mw	2.657	mw	2.652	1
132; 20$\bar{4}$	2.602	ms	2.597	m	2.600	1
13$\bar{4}$; 202	2.550	m	2.550	mw	2.560	1
0, 0, 12; 13$\bar{6}$; 204	2.392	ms	2.392	ms	2.395	1
136; 20$\bar{8}$	2.277	vvw	2.266	vvw	—	—
13$\bar{8}$; 206	2.209	vvw	2.214	vw	2.204	1
138; 2, 0, $\bar{10}$	2.082	w	2.081	w	2.083	1
0, 0, 14	—	—	2.048	vw	2.049	1
208	2.016	w	2.011	vw	2.016	1
1, 3, $\bar{12}$; 2, 0, 10	1.835	vvw	1.835	vvw	1.833	1
2, 0, $\bar{14}$	1.744	mw	1.748	w	1.745	1
1, 3, $\bar{14}$; 2, 0, 12	1.673	mw	1.677	mw	1.676	1
1, 3, 14; 2, 0, $\bar{16}$	1.576	vvw	1.574	vvw	1.584	1
060; 1, 3, $\bar{16}$; 2, 0, 14; 330; 332; 334	1.537	s	1.537	ms	1.540	1
332; 33$\bar{6}$	1.506	vvw	1.508	vvw	—	—
0, 0, 20; 1, 3, 16; 2, 0, 18	1.444	vw	1.449	w	1.447	1
338	1.356	vw	1.357	vw	1.361	—
1, 3, 18; 2, 0, $\bar{20}$ 3, 3, $\bar{12}$; 40$\bar{2}$	1.332	mw	1.334	mw	1.331	1
2, 0, $\bar{20}$; 400; 40$\bar{6}$	1.319	mw	1.320	mw	—	—
1, 3, 20; 2, 0, 18; 3, 3, 14; 402	1.296	w	1.298	w	1.294	—
404	1.278	w	1.275	vw	—	—

* After Walker (1961).

present. A plot of the relative intensity (peak height basis) of six progressive orders of the 002 peak of 14.5 Å for some of the fractions is shown in Fig. 1. In the finer fractions the relative intensities of the higher order reflections show a progressive decrease in intensity. In the finest fraction the relative intensities of successive orders are not similar to the typical continuous increase from the 004 to the 0, 0, 10 of a true vermiculite.

The same slides that were used in the 00l oriented scans were subjected to ethylene glycol treatment. The slides were placed in an atmosphere

saturated with ethylene glycol vapor at 60°C and a minimum of 8 hr was allowed for complete expansion. X-ray diffractometry was carried out from 2° to 65° 2θ. Check scans were made over the 002 peak after a complete run to make sure that a collapse of the expanded material had not occurred during the time the complete scan was being made.

TABLE 2.—X-RAY DATA FOR SELECTED SAMPLES OF SIZE-FRACTIONED LLANO VERMICULITE

Indices	Particle size (microns) 16–32 d(Å)	4–8 d(Å)	1–2 d(Å)	$\frac{1}{4}$–$\frac{1}{2}$ d(Å)
002	14.52	14.40	14.40	14.50
004	7.22	7.20	7.20	7.31
006	4.77	4.78	4.80	—
02l; 11l	4.61	4.61	4.69	4.50
008	3.60	3.59	3.60	3.60
0, 0, 10	2.890	2.862	2.878	2.89
130; 100; 20$\bar{2}$	2.656	2.636	2.648	—
132; 204	2.596	2.593	—	—
13$\bar{4}$; 202	2.557	2.553	2.550	2.564
0, 0, 12; 13$\bar{6}$; 204	2.397	2.392	2.392	—
138; 2, 0, $\bar{1}$0	2.084	—	—	—
0, 0, 14	2.058	—	—	—
208	2.020	—	—	—
1, 3, $\bar{1}$4; 2, 0, 12	1.680	—	—	—
060; 1, 3, $\bar{1}$6; 2, 0, 14; 330; 332; 334	1.537	1.537	1.535	—
0, 0, 20; 1, 3, 16; 2, 0, $\bar{1}$8	1.450	—	—	—
1, 3, 18; 2, 0, $\bar{2}$0; 3, 3, 12; 402	1.334	—	—	—

The $\frac{5}{10}$0–$\frac{1}{10}$ micron fraction undergoes an almost complete expansion to 16.5 Å. A slight shoulder on the peak at about 6° 2θ also suggests that some material did not undergo ethylene glycol expansion. This becomes more apparent in the coarser particle size fractions.

An approximation of the per cent of expandable material present in each size-fraction was made by measuring the decrease in the height of the 14.5 Å peak after ethylene glycol treatment. The results of these data are plotted in Fig. 2 as per cent decrease in intensity of the 002 peak versus particle size. This indicates that the per cent of expandable material varies from 87% in the $\frac{5}{10}$0–$\frac{1}{10}$ micron fraction to 30% in the 16–32 microns fraction.

https://doi.org/10.1346/CCMN.1967.0150116 Published online by Cambridge University Press

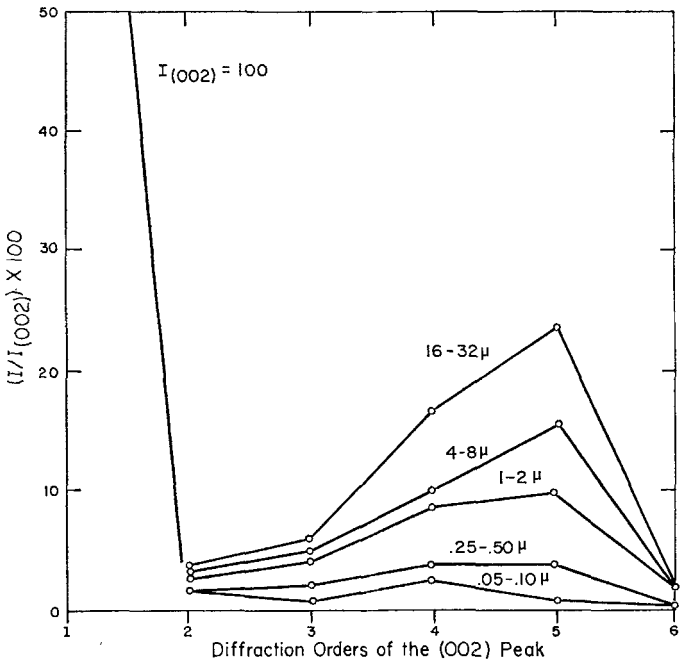

FIG. 1. Relative intensities of orders of the 002 peaks for the size-fractioned Llano vermiculite. Based on peak height measurements of 00*l* oriented sample X-ray data.

DIFFERENTIAL THERMAL ANALYSIS

Figure 3 contains the DTA curves of all samples run at 10°C per minute from room temperature to 1020°C. All samples have an endothermic doublet in the 100–250°C range. This doublet marks the loss of interlayer water and is not well resolved in the finer fractions as in the coarser materials. This is interpreted as a reflection of the lower interlayer magnesium content of the smaller crystallites. The endotherms at 500–600°C and at 700–900°C indicate the loss of water due to a breakdown of the octahedral cation to hydroxyl bond. The exotherms at 800–900°C represent the formation of clinoenstatite as determined by X-ray diffraction scans of samples that were heated to 1000°C.

CHEMICAL ANALYSES

Partial quantitative chemical analyses were obtained by X-ray fluorescence spectroscopy. The results are listed in Table 3 and compared with two analyses of vermiculite from the same locality provided by Barnes and

https://doi.org/10.1346/CCMN.1967.0150116 Published online by Cambridge University Press

Clabaugh (1961), which were analyzed by the Minnesota Rock Analysis Laboratory, Minneapolis. The agreement is fairly reasonable, considering that the analyses were not run on cuttings of the same material. Analysis by X-ray fluorescence of the large crystals (ground to −400 mesh) shows a higher silica and iron oxide content and a lower magnesia and alumina content than the two analyses from the guidebook. Analyses of the size-fractioned

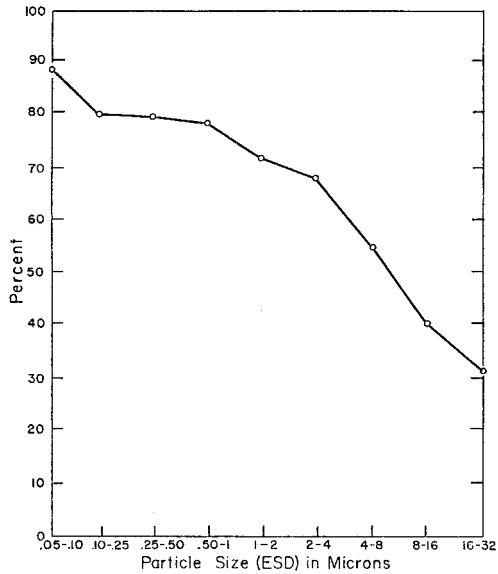

FIG. 2. Per cent reduction in height of the 002 peak of size-fractioned vermiculite samples after ethylene glycol treatment.

material indicate a progressive increase of SiO_2, Fe_2O_3, and K_2O, and a decrease in the MgO content from the coarser (16–32 microns) to the finer ($\frac{1}{10}$–$\frac{1}{4}$ micron) fractions. Variations in Al_2O_3 are considered within the precision range of the X-ray fluorescence techniques. Analyses of Na_2O, MnO, F, and Cl were not determined by X-ray fluorescence, and all iron was reported as Fe_2O_3. Figure 4 is a graphical illustration of the analyses listed in Table 3 calculated on the basis of weight per cent of oxides on a 1000°C fired basis. Only the oxides of the more significant constituents, silicon, aluminum, iron, and magnesium, are included.

STRUCTURE

The various chemical constituents from the analyses reported in Table 3 were partitioned into a three-layer mica lattice using the method described by Marshall (1949). The results are listed in Table 4 on a half unit-cell basis (22 charges). There were no available means of determining the relative ratio

of ferric to ferrous iron present, therefore, calculations were made twice. Row 1 considers all iron as Fe^{3+} and row 2 considers all iron as Fe^{2+}. From the analyses provided by Barnes and Clabaugh (1961) listed in Table 3, the iron seems to be predominantly in the higher oxidation state and it is thought that calculations on this basis represent a closer approximation to the actual structural formula. Structural formulae are also written on the assumption that the octahedral layer does not contain more than six positive charges

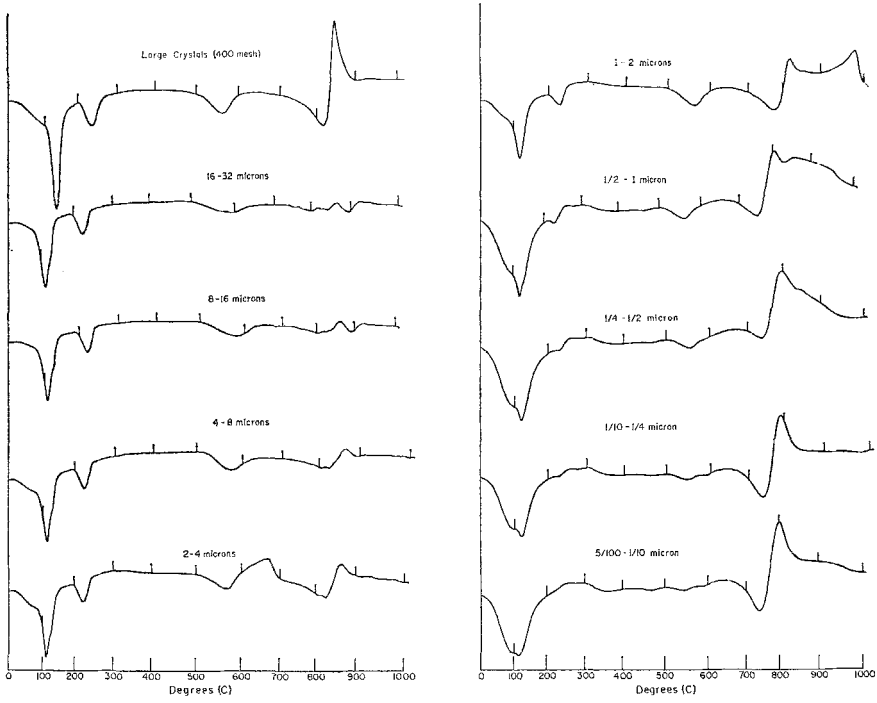

FIG. 3. Differential thermal analysis patterns of Llano vermiculite samples.

(half unit-cell basis). This assumption may not be strictly valid, but it provides a common basis for directly comparing the calculated structural formulae of the various particle sizes.

The data in Table 4 indicate that the aluminum for silicon substitution in the tetrahedral layer decreases with decreasing particle size. In the octahedral layer magnesium is observed to decrease with decreasing particle size, whereas iron and aluminum increase. The titanium content is relatively constant throughout the range of particle sizes. The total surface charge and interlayer cation content are also observed to decrease with the size of the

https://doi.org/10.1346/CCMN.1967.0150116 Published online by Cambridge University Press

TABLE 3.—CHEMICAL ANALYSES OF LLANO VERMICULITES (CARL MOSS RANCH)

	Guidebook*		Analyses by X-ray fluorescence								
	Sample 1	Sample 2	Sample A	B-1	B-2	B-3	B-4	B-5	B-6	B-7	B-8
SiO_2	35.19	34.95	39.03	40.96	41.50	41.82	42.16	42.07	43.67	44.33	44.27
Al_2O_3	12.73	12.85	9.16	8.45	8.16	8.18	8.18	8.13	8.39	8.20	8.13
TiO_2	0.75	0.13	1.03	0.50	0.54	0.54	0.55	0.51	0.42	0.42	0.37
Fe_2O_3	3.52	3.09	4.95	6.49	6.96	7.87	8.59	9.60	12.91	13.79	13.75
FeO	0.46	0.57	—	—	—	—	—	—	—	—	—
MnO	0.05	0.03	—	—	—	—	—	—	—	—	—
MgO	26.85	29.25	24.01	22.31	21.93	20.01	18.68	15.70	10.47	8.99	9.22
CaO	0.24	0.00	0.11	0.57	0.56	0.43	0.41	0.39	0.41	0.44	0.45
Na_2O	0.02	0.02	—	—	—	—	—	—	—	—	—
K_2O	0.01	0.03	0.05	0.09	0.17	0.20	0.21	0.20	0.30	0.32	0.35
H_2O^+	10.77	10.87	9.55	8.55	8.42	8.88	10.18	9.89	9.97	9.91	9.85
H_2O^-	9.00	7.55	10.14	9.72	9.62	9.65	8.53	10.76	10.78	10.81	10.75
F	0.15	0.38	—	—	—	—	—	—	—	—	—
Cl	0.04		—	—	—	—	—	—	—	—	—
Total	99.78	99.72	98.03	97.73	97.86	97.58	97.49	97.25	97.32	97.21	97.14

* From Barnes and Clabaugh (1961).

Legend: Sample A refers to the large yellow crystals that were ground to 400 mesh. Samples B refer to the size-fractioned vermiculite, particle sizes 16–32 (B-1), 8–16 (B-2), 4–8 (B-3), 2–4 (B-4), 1–2 (B-5), $\frac{1}{2}$–1 (B-6), $\frac{1}{4}$–$\frac{1}{2}$ (B-7), and $\frac{1}{10}$–$\frac{1}{4}$ (B-8) microns (ESD).

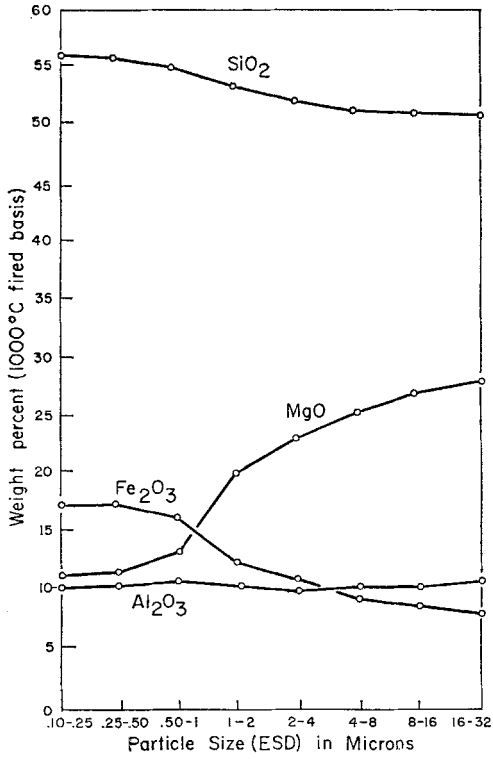

FIG. 4. Partial chemical data for size-fractioned vermiculite. Based on quantitative analyses by X-ray fluorescence.

particles. This is predominantly a function of the variation in interlayer magnesium. The calcium and potassium contents are relatively constant on an ion for ion basis.

The data in Table 4 have been plotted graphically in Fig. 5 for ease of examination. Figure 5A shows the variation in the Al/Si of the tetrahedral layer with particle size. For comparison purposes dashed lines have been added that show the Al/Si ratio for batavite and a vermiculite from West Chester, Pennsylvania, provided by Walker (1961). Also represented by dashed lines are the results of Marshall calculations on the analysis of sample 1 (from the guidebook) and the large crystals of Llano vermiculite from the Carl Moss Ranch which were ground to −400 mesh and analyzed by X-ray fluorescence techniques.

Figure 5B is an illustration of the total ion content in the octahedral layers. Again dashed lines represent data for above mentioned samples.

Figure 5C is a triangular plot showing the contribution of each ionic constituent to the total composition of the octahedral layer. Data for the

https://doi.org/10.1346/CCMN.1967.0150116 Published online by Cambridge University Press

TABLE 4.—RESULTS OF STRUCTURE CALCULATIONS ON CHEMICAL ANALYSES OF THE SIZE-FRACTIONED LLANO VERMICULITE

		Tetrahedral		Octahedral				Number octahedral	Interlayer cations		
ESD	*	Si	Al	Mg	Fe	Al	Ti	cations	Mg	Ca	K
16–32	1	3.24	0.76	2.31	0.38	0.04	0.03	2.77	0.32	0.05	0.01
	2	3.30	0.70	2.38	0.39	0.11	0.03	2.91	0.30	0.05	0.01
8–16	1	3.27	0.73	2.28	0.41	0.03	0.03	2.75	0.30	0.05	0.02
	2	3.34	0.66	2.36	0.41	0.11	0.03	2.90	0.27	0.05	0.02
4–8	1	3.33	0.67	2.09	0.47	0.10	0.03	2.69	0.28	0.04	0.02
	2	3.40	0.60	2.19	0.48	0.18	0.03	2.88	0.25	0.04	0.02
2–4	1	3.37	0.63	1.95	0.52	0.14	0.03	2.64	0.27	0.04	0.02
	2	3.45	0.55	2.05	0.53	0.24	0.03	2.85	0.23	0.04	0.02
1–2	1	3.45	0.55	1.69	0.59	0.24	0.03	2.55	0.23	0.04	0.02
	2	3.55	0.45	1.79	0.61	0.36	0.03	2.79	0.18	0.04	0.02
½–1	1	3.60	0.40	1.18	0.80	0.41	0.03	2.37	0.15	0.04	0.02
	2	3.73	0.27	1.24	0.83	0.58	0.03	2.68	0.09	0.04	0.03
¼–½	1	3.66	0.34	0.97	0.85	0.45	0.03	2.31	0.13	0.04	0.03
	2	3.80	0.20	1.10	0.89	0.63	0.03	2.65	0.05	0.04	0.04
1/10–¼	1	3.65	0.35	1.02	0.85	0.44	0.02	2.33	0.11	0.04	0.03
	2	3.80	0.20	1.14	0.89	0.62	0.02	2.67	0.04	0.04	0.03

* 1 = Fe^{3+}; 2 = Fe^{2+}.

West Chester vermiculite, batavite, and Llano vermiculite (guidebook analysis) are represented. Points 4 through 9 are from calculations based on the data in Table 3. Point 4 represents the large crystals (ground to −400 mesh) analyzed by X-ray fluorescence, and points 5 through 9 are for the 16–32, 4–8, 1–2, ½–1, and 1/10–¼ micron fractions where all iron is considered as Fe^{3+}. Titanium is not included here, nor is provision made for the differences in the total number of ions in the octahedral layer. The change in composition from the coarser-size fraction through to the finer material is toward a nontronitic chemical composition.

CATION EXCHANGE CAPACITY

Theoretical cation exchange capacities were calculated for all particle sizes of the size-fractioned material. These are presented in Fig. 6 as two curves. Curve A shows the calculations from Table 4, rows numbered 1, in which all iron is considered as Fe^{3+}. Curve B is from data in the same table, but from rows numbered 2 where all iron is considered as Fe^{2+}.

The cation exchange capacities of the 16–32, 4–8, 1–2, ½–1, ¼–½, 1/10–¼ micron samples were measured by the sodium hydroxide continuous titration technique. Figure 6, curve C, shows the data that were obtained from this series of measurements. No claim is made as to the completeness of the exchange reaction in any sample. It is known from X-ray diffraction and

https://doi.org/10.1346/CCMN.1967.0150116 Published online by Cambridge University Press

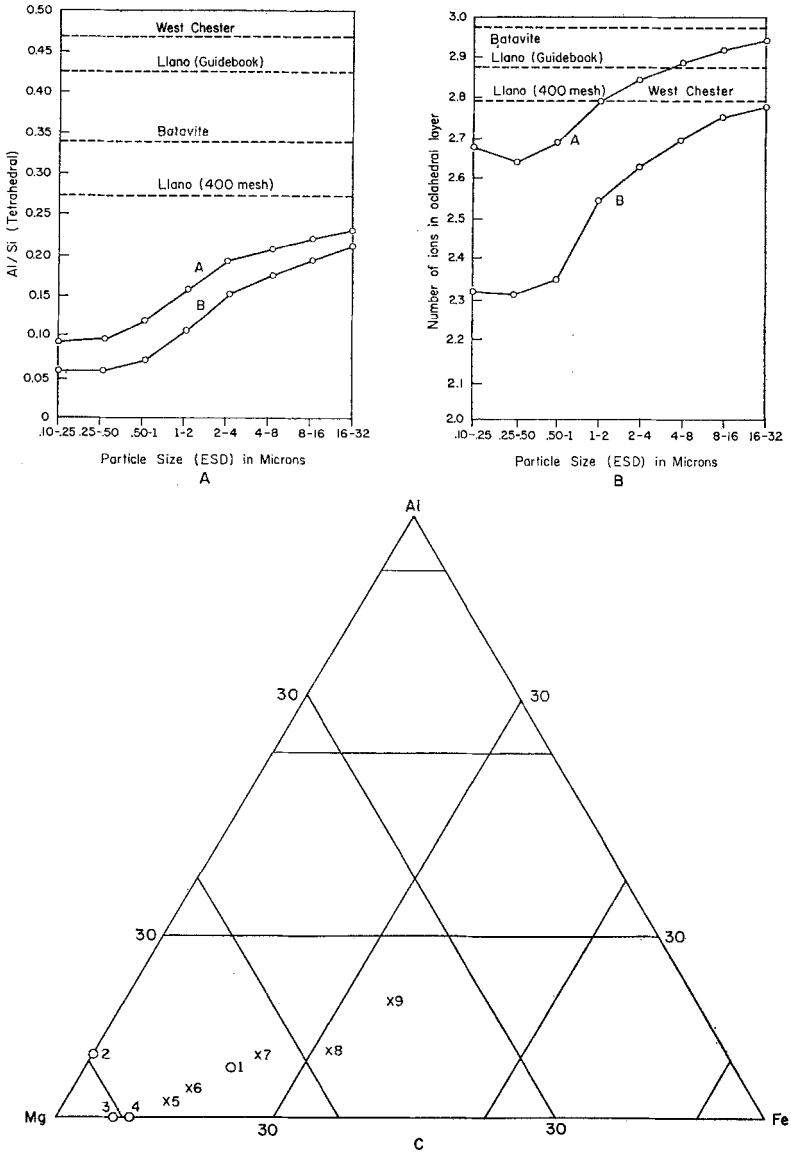

FIG. 5. (A) Tetrahedral layer compositions of selected vermiculites and size-fractioned Llano vermiculite. Curve A: All iron considered as Fe^{3+}. Curve B: All iron considered as Fe^{2+}. (B) Total ion content of octahedral layer of selected vermiculites and size-fractioned Llano vermiculite. Curve A: All iron considered as Fe^{2+}. Curve B: All iron considered as Fe^{3+}. (C) Octahedral layer population of selected vermiculites. 1. West Chester; 2. Batavite; 3. Llano (Guidebook); 4. Llano (−400 mesh); 5–9. Size-fractioned Llano vermiculite: 5. 16–32 microns, 6. 4–8 microns, 7. 1–2 microns, 8. $\frac{1}{2}$–1 micron, 9. $\frac{1}{10}$–$\frac{1}{4}$ micron.

https://doi.org/10.1346/CCMN.1967.0150116 Published online by Cambridge University Press

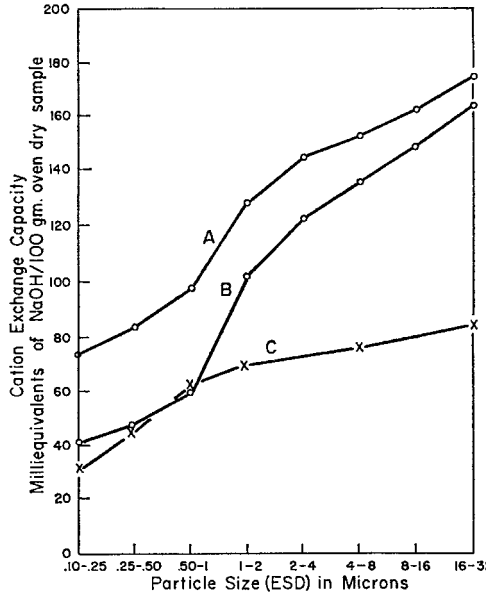

FIG. 6. Calculated and measured cation exchange capacities of particle size fractions of Llano vermiculite. Curve A: CEC calculated, iron considered as Fe^{3+}. Curve B: CEC calculated, iron considered as Fe^{2+}. Curve C: CEC measured.

DTA analyses that the exchange was only about one-third effected in the 16–32 microns material and about one-half completed in the 4–8 microns fraction. It is thought that the cation exchange capacity did approach completeness in the finer fractions.

Whether or not the cation exchange capacity data represent total exchange, they are of significant value. The variation in cation exchange shows a trend from high values to low values with decreasing particle size which agrees with the trend predicted from the calculated structures. This provides independent evidence supporting the calculations as good approximations of actual structural formulae.

INTERPRETATIONS

X-ray diffraction data provide evidence that the smaller size fractions (less than 1 micron ESD) of the vermiculite regolith from the Carl Moss Ranch in Llano, Texas, are not true vermiculites. The *b*-axis parameter of the coarser fractions, calculated from the *d*-values of the 060 peaks, ranges from 9.21 Å to 9.24 Å attesting to the trioctahedral nature of these materials. In the less than 1 micron samples the 02*l*, 11*l* edge appears at 19.7° 2θ (4.50 Å). An approximate *b*-axis parameter based on these data is 9.00 Å, which is to be expected for dioctahedral micas.

https://doi.org/10.1346/CCMN.1967.0150116 Published online by Cambridge University Press

The structural formulae calculated from chemical analyses indicate a more dioctahedral composition for the smaller-sized particles. Independent data support these as reasonably good approximations of the actual average structural formulae. Differential thermal analyses show that the interlayer magnesium content is higher in the coarser fraction and decreases with particle size. Although calculated and measured values for the cation exchange capacities are not in close agreement, they do show the same variation with particle size. The measured CEC decreased with particle size at the same relative rate as values predicted from the calculated structural formulae. Disagreements in CEC values may be primarily the result of fundamental assumptions made for the purpose of standardizing the structural formula calculations. If more magnesium were placed in the octahedral layer, the predicted cation exchange capacities would be somewhat lower. Good CEC data were not obtainable for the larger particles because of the difficulty in approaching a total exchange condition. This is primarily due to incomplete conversions of the coarser-grained vermiculite to the hydrogen form. This could be accomplished if a more rigorous acid treatment were employed. However, this could result in a partial removal of lattice elements as well as interlayer cations and further complicate the interpretation of total cation exchange capacity information.

The heterogeneity of the vermiculite regolith may be predominantly due to a mechanical mixture of distinct phases, each crystallite being fairly homogeneous and crystallite compositions being quite different, but varying within the ranges of two or more distinct modal types. For simplicity's sake, the system may be considered as discrete particles of two end members with the trioctahedral crystallites occupying a coarser particle size distribution and the dioctahedral crystallites concentrated in the smaller-size class. If this is the case, the data may simply be an expression of the higher degree of stability of dioctahedral micas with respect to trioctahedral types in a weathering environment.

An alternative is that the heterogeneity of this material is one of mixed domains within individual crystals. In this case it might be reasoned that one phase (dioctahedral type) is an alteration product of the other (trioctahedral type) phase. A "reaction-rim" of fairly constant thickness may exist around an essentially unaltered core. This "reaction-rim" would become increasingly more significant volumetrically as the size of the affected particle was decreased. At some lower-size limit, the depth of alteration would result in a completely altered phase. That is, the crystallite would be fairly homogeneous and of a composition similar or identical to the "reaction-rim" of the larger crystallites.

Arguments supporting both alternatives may be equally justified by interpretations of the data presented in this study. The difficulty lies in the fact that the properties observed, measured, and calculated in all cases are average properties of the mixture of two or more phases. Final conclusions become even more difficult to draw if the system is considered as more than

a simple two-phase mixture. However, the systematic variation in the chemical composition with particle size suggests that a direct correlation may be made using these parameters. It is probably a justified assumption that the finer-grained material is, indeed, an alteration product of the coarser-grained material. Therefore, the following discussion attempts to discuss the process by which the trioctahedral type of vermiculite may well be expected to alter to a dioctahedral phase similar in composition and properties to that of the fine-grained material.

Weaver (1958) pointed to the inadvisability, or at least the problems, involved in classifying clay minerals on the basis of secondary properties such as swelling. As pointed out by Jonas (1960) these properties are a function of the chemical and physical properties of a particular crystal. If these are, in turn, a function of particle size, then care should be taken in the assignment of mineral names that would subdivide into separate mineral groups or species, substances that are basically the same. Using principles of crystal chemistry, Jonas described the possibility of differences in chemical composition that might occur at the boundaries of mineral grains. Referring to the work of Pauling (1948) and data provided by Fyfe (1951), Jonas suggested that the differences in the bond character (per cent ionic), as estimated from electronegativity differences of various cations with respect to oxygen, would lead to some interesting reactions at the grain surfaces in an aqueous environment. Under such conditions those cations, in equivalent structural positions, having a higher degree of ionic bond character could be preferentially dissolved and removed from the lattice. The more commonly occurring cations in clay and mica structures may be arranged in order of decreasing per cent of ionic bond character, $Mg > Al > Fe^{2+} > Si$. Iron as Fe^{3+} and silicon are approximately the same. In the tetrahedral layer, then, it might be expected that aluminum ions could be preferentially dissolved with respect to silicon. At exposed octahedral sites a depletion of magnesium could occur with respect to iron and aluminum ions. Iron would be expected to be preferentially retained in equivalent positions with respect to aluminum.

On this basis, Jonas proposed that such differences in chemical composition at the grain boundaries are negligible when dealing with large macroscopic crystals. As the particle size diminished, however, these non-uniform compositional features might affect the overall properties of the substance. Some of the differences between montmorillonite and muscovite may be attributed to such a phenomenon. These would be the lower tetrahedral Al/Si ratio and the lower average surface charge density of the montmorillonites. Jonas (1960), therefore, proposed a model for montmorillonite consisting of an interior with a mica composition and a different composition at the edge.

This same approach can be followed to explain the differences between the structure, chemical composition and properties of the larger and smaller particles of the vermiculite regolith. Preferential solution of cations from equivalent lattice positions by hydrothermal and/or weathering activity could adequately account for observed differences. The Al/Si ratio of the

tetrahedral layer was shown to decrease systematically with particle size (Fig. 5). Selective removal of magnesium and an increase in the iron and aluminum content in the octahedral layer are also consistent with this argument. The total effect is one in which the material is altered from a trioctahedral to a more dioctahedral type of structure.

A secondary effect is a relocation of part of the charge deficiency in the octahedral layer. The total surface charge is also decreased and this affects the cation exchange capacity and the low-temperature characteristics of the DTA pattern. The low surface charge density and the transferral of part of the lattice charge sites to the octahedral layer, thus creating a weaker lattice to interlayer cation bond, probably account for the more expandable nature of the smaller particles with ethylene glycol treatment.

REFERENCES

BARNES, V. E., and CLABAUGH, S. E. (1961) Vermiculite deposits near Llano, Texas: *Texas Univ., Guidebook* **3**, 45–53.

CLABAUGH, S. E., and BARNES, V. E. (1959) Vermiculite in central Texas: *Texas Univ., Rep. of Invest.* **40**, 32 pp.

FYFE, W. S. (1951) Isomorphism and bond type: *Amer. Min.* **36**, 538–42.

JONAS, E. C. (1960) Mineralogy of the micaceous clay minerals: *Proc. Internat. Comm. Study Clays*, Copenhagen, 1–16.

JONAS, E. C. (1963) Ion exchange at edge and interlayer in montmorillonites differing in size: *Science* **140**, 75–6.

JONAS, E. C., and ROBERSON, H. E. (1960) Particle size as a factor influencing expansion of the three-layer clay minerals: *Amer. Min.* **45**, 828–38.

MARSHALL, C. E. (1949) *The Colloid Chemistry of the Silicate Minerals:* Academic Press, New York, 195 pp.

PAIGE, S. (1912) Description of the Llano and Burnet quadrangles: *U.S. Geol. Surv. Geol. Atlas, Llano-Burnet Folio* (No. 183), 16 pp.

PAULING, L. (1948) *The Nature of the Chemical Bond*: Cornell University Press, Ithaca, New York.

ROBERSON, H. E., and JONAS, E. C. (1965) Clay minerals intermediate between illite and montmorillonite: *Amer. Min.* **50**, 766–70.

WALKER, G. F. (1961) Vermiculite minerals, Chap. VII in *X-ray Identification and Crystal Structures of Clay Minerals*: Mineralogical Society, London.

WEAVER, C. E. (1958) The effects and geologic significance of potassium "fixation" by expanding clay minerals derived from muscovite, biotite, chlorite, and volcanic material: *Amer. Min.* **43**, 839–61.